Optimum Reconfiguration of Droop-Controlled Islanded Microgrids

Morad Mohamed Abdelmageed Abdelaziz, *Member, IEEE*, Hany E. Farag, *Member, IEEE*, and Ehab F. El-Saadany, *Senior Member, IEEE*

***Abstract*—This paper proposes a new formulation for the optimum reconfiguration of islanded microgrid (IMG) systems. The reconfiguration problem is casted as a multi-objective optimization problem, in order to: 1) minimize the IMG fuel consumption in the operational planning horizon for which islanded operation is planned; 2) ensure the IMG capability to feed the maximum possible demand by enhancing its voltage instability proximity index taken over all the states at which the islanded system may reside; and 3) minimize the relevant switching operation costs. The proposed problem formulation takes into consideration the system's operational constraints in all operating conditions based on the consideration of the uncertainty associated with renewable resources output power and load variability. Moreover, the proposed formulation accounts for droop controlled IMG special operational characteristics as well as the availability/unavailability of a supervisory microgrid central controller (MGCC). The formulated problem is solved using non-dominated sorting genetic algorithm II (NSGA-II). MATLAB environment has been used to test and validate the proposed problem formulation. The results show that the implementation of appropriate IMG reconfiguration problem formulations will enhance the performance of IMG systems and facilitate a successful integration of the microgrid concept in distribution networks.**

***Index Terms*—Distributed generation, distribution network reconfiguration, droop control, islanded microgrids, renewable energy resources.**

I. Introduction

MOTIVATED by different technical and economic benefits, the electric power distribution networks are currently moving towards accommodating higher penetration levels of renewable and distributed generation (DG) units. The increased application of renewable and DG technologies is creating microgrids, within the electric power distribution networks, with sufficient generation capacities to feed most or all of their local loads [1]. Such microgrids can operate in grid-connected and islanded modes i.e., in parallel to and isolated from the main grid, respectively. The operation of microgrids in islanded mode brings numerous benefits to both customers and utilities. The recent IEEE standard 1547.4 enumerates several potential benefits for the islanded microgrid (IMG) operation. Such benefits include: 1) improving customers' reliability, 2) relieving electric power system overload problems, 3) resolving power quality issues, and 4) allowing for maintenance of the power system components without interrupting customers. These benefits motivate the operation of microgrid systems in the islanded mode. As such, the connection between a microgrid and its upstream main grid might be arbitrary open [1]. Consequently, the time span of IMG operation is expected to be long enough to mandate a detailed consideration of the IMG operational planning studies.

In islanded mode of operation, the DG units forming the IMG must be controlled such that: 1) it achieves appropriate sharing of the load demands among the DG units in the IMG, and 2) it controls the IMG voltage and frequency regulation. The majority of DG units in microgrids are interfaced through a voltage-source converter coupled with a passive output filter [2], [3]. In order to accommodate this type of DG interface with the requirements of IMG operation, two operating schemes have been proposed in the literature; namely master-slave and droop control schemes. Master-slave control schemes are based on the availability of high bandwidth communication links that communicate the dynamic power sharing signals among the DG units in the island. In most cases, due to its communication infrastructure dependency, master-slave control schemes are found to be both costly and unreliable in the case of distribution system IMGs [3]. On the other hand, droop control schemes depend on locally measured values to mimic the behavior of synchronous generators operating in parallel and hence attain appropriate sharing of the load demand among the different DG units in the IMG, while controlling the IMG voltage and frequency regulation [4].

Motivated by the anticipated long time spans of IMG operation, different new formulations have been put forward in the literature for the operational planning studies of IMG systems, taking into account the aforementioned droop-controlled IMG special operational characteristics [4]–[13]. In [4]–[6], detailed power flow analysis algorithms have been proposed for IMG systems. In [7] and [8], the operation of IMG systems is optimized to minimize the overall island fuel consumption. In [9], a different multistage optimal power flow (OPF) algorithm was presented to minimize the IMG fuel consumption while considering the system losses and operational constraints. In [10] and [11], the IMG emissions are minimized along with the system fuel consumption. In [12], an energy management structure has been proposed to optimize the operation of IMG in the presence of stochastic renewable resources. Yet, all the previous work in

Manuscript received November 24, 2014; revised March 05, 2015, May 27, 2015, and July 10, 2015; accepted July 12, 2015. Date of publication August 04, 2015; date of current version April 15, 2016. Paper no. TPWRS-01612-2014.

M. M. A. Abdelaziz is with Western Washington University, Engineering and Design, Bellingham, WA 98225 USA (e-mail: morad.abdelaziz@wwu.edu).

H. E. Z. Farag is with York University, Electrical Engineering and Computer Science, Toronto, ON M3J 1P3, Canada (e-mail: hefarag@cse.yorku.ca; haniissa2001@yahoo.com).

E. El-Saadany is with the University of Waterloo, Electrical and Computer Engineering Department, Waterloo, ON N2L3G1, Canada (e-mail: ehab@uwaterloo.ca).

Digital Object Identifier 10.1109/TPWRS.2015.2456154

the literature assumed that the topological structure of an IMG system is predetermined. However, given the anticipated long time span of intentional IMG operation [1], there is a need to consider the optimal reconfiguration of distribution networks IMGs which will facilitate a seamless integration of the microgrid concept in electric distribution networks. The appropriate reorganization of a distribution network as it operates in the islanded mode can bring significant benefits to both customers and utilities, with the opportunity of reducing energy costs and increasing the perceived reliability.

Distribution network reconfiguration is the processes of changing the topological structure of distribution feeders by updating the open/close status of the network sectionalizes and tie switches. Reconfiguration is an effective way to improve the electrical power distribution network performance by selecting the switches states that can achieve the maximum improvement in the system operating conditions while satisfying the system operational constraints [13]–[16]. In [13], a distribution network reconfiguration approach is proposed to maximize the system loadability. In [14], a reconfiguration heuristic is presented to reduce the distribution network total power loss and its maximum branch current. References [15] and [16] present different reconfiguration approaches for distribution systems operating in the presence of DG units. Yet, even though distribution network reconfiguration has been studied extensively in the literature, so far there is no reconfiguration approach that takes into account the special features and operational characteristics of droop controlled IMG systems.

The optimal reconfiguration of droop-controlled IMGs should: 1) ensure the satisfaction of the system operational constraints in all operating conditions at which the islanded system may exist based on the consideration of the uncertainty and variability associated with the output power of renewable DG as well as the load variability; 2) minimize the IMG fuel consumption in the operational planning horizon for which the IMG operation is planned; 3) ensure the IMG capability to feed the maximum possible demand by enhancing its voltage instability proximity index taken over all the states in which the islanded system may reside; 4) account for the switching operation costs and balance the benefits of the reconfiguration process against the cost of switching; 5) account for the droop controlled IMG special operational characteristics and the models used to represent it; and 6) account for the availability/unavailability of a supervisory microgrid central controller (MGCC) and its associated communication infrastructure.

Based on these considerations, this paper proposes a new probabilistic formulation for the optimal reconfiguration of droop-controlled IMG systems. The proposed formulation uses the IMG topology as a control variable in order to maximize the IMG loadability limits while minimizing the island's fuel consumption and the number of switching operations required to implement the optimal topology. The problem of IMG reconfiguration is accordingly casted as a multi-objective optimization problem to deal with the trade-off between the three objectives at stake. The solution of the proposed optimization problem entails finding the non-dominated set of solutions representing the best possible trade-offs between the three objectives under consideration. Such non-dominated solutions constitute the so-called Pareto optimal set. The values of the objective functions corresponding to the elements of the Pareto optimal set represent the so-called Pareto front. The proposed multi-objective optimization problem formulation is solved using the non-dominated sorting genetic algorithm II (NSGA-II) in order to obtain radial topologies of distribution system IMGs within a Pareto front. This work accounts for the operational philosophy and constraints of droop-controlled IMG systems, the stochastic nature of the system generation and loads, and the availability/unavailability of MGCC.

II. Proposed Problem Formulation

This section presents the proposed multi-objective optimal feeder reconfiguration problem formulation for droop-controlled IMG systems. The objectives in the proposed formulation are to minimize the IMG fuel consumption, maximize the IMG loadability limits, and minimize the number of switching operations required. The proposed problem formulation reflects the droop-controlled IMG special features by: 1) employing a probabilistic analytical approach to account for the stochastic nature of the IMG generation and demand; 2) adopting a set of power flow equations that reflects the operational characteristics of droop controlled IMG systems; and 3) accounting for the availability/unavailability of a MGCC. Moreover, the proposed formulation accounts for the system operational constraints by: 1) ensuring that the bus voltages and branch currents are within their specified limits, 2) feeding all load points in the system, 3) asserting that the system structure after reconfiguration remains radial to provide easy transition of IMGs to grid-connected mode, and 4) implementing a set of nonlinear complementary constraints to model the behavior of droop-controlled DG units as they reach their maximum generation capability. In the following subsections, the main characteristics and mathematical details of the proposed formulation are presented and discussed.

A. Probabilistic Model

Given the stochastic nature of both generation and demand in typical IMG systems, a combined generation load model is analytically developed to describe all possible microgrid states and their respective probabilities. This analytical approach has been previously validated by comparison with Monte Carlo simulations (MCS) in [17]. Assuming that the probabilities of the gross generation states, unaltered by the load at the same node, in the operational planning horizon $\rho_G^{st}\left\{N_G^{st}\right\}$ are independent on the probabilities of the gross load states $\rho_L^{st}\left\{N_L^{st}\right\}$, the probabilities of IMG states $\rho_{IMG}^{st}\left\{N_{IMG}^{st}\right\}$ describing different possible combination of generation and load states can be obtained by convolving their respective probabilities as follows:

$$\rho_{IMG}^{st}\left\{N_{IMG}^{st}\right\} = \rho_G^{st}\left\{N_G^{st}\right\} * \rho_L^{st}\left\{N_L^{st}\right\} \quad (1)$$

where $\left\{N_G^{st}\right\}$ is the set of all possible generation states, $\left\{N_L^{st}\right\}$ is the set of all possible load states, and $\left\{N_{IMG}^{st}\right\}$ is the set of all possible IMG states. Based on this concept, the generation load model for the IMG can be obtained by listing all possible combinations of generation output power states and load states. Similarly, the different generation states are composed by convolving generation states probabilities based on the state model of each type of DG units. For two DG units G_1 and G_2, with different state models, the model of the combined generation states can be obtained as follows:

$$\rho_G^{st}\left\{N_G^{st}\right\} = \rho_{G_1}^{st}\left\{N_{G_1}^{st}\right\} * \rho_{G_2}^{st}\left\{N_{G_2}^{st}\right\}. \quad (2)$$

Generation states model for variable power DG units are calculated by dividing the continuous probability density function (PDF) into several states. For instance, the generation states model of wind-based DG units can be extracted by dividing the wind speed PDF into several states with a step of 1 m/s [17]. As such the probability of a wind state "i" can be calculated as follows:

$$\rho_i^{wind} = \int_{v_{\min,\, i}}^{v_{\max,i}} f(v)\,.dv \quad (3)$$

where $f(v)$ is the distribution probability of wind speed, $v_{\min,i}$ and $v_{\max,i}$ are the wind speed limits of state "i". Similar approaches can be used for other renewable power resources. The detailed procedures for the generation of the PDF's for the renewable resources and load as well as for the calculation of the output power of renewable generation resources corresponding to each state can be found in [17] and [18].

Irrespective of the IMG control and configuration, an island can be successful if and only if there is enough generation to match the island total demand. Accordingly, amongst the set of all possible IMG states, only the set of states with sufficient generation to meet its respective demand are considered in the proposed formulation i.e.,; the set of admissible microgrid states. Based on the generation load model described above, the necessary condition for an IMG state st to be admissible is given as follows:

$$\sum_{i\in B} S_{Gi,\max}^{st} \geq \sqrt{\left(\sum_{i\in B} P_{Li}^{st}\right)^2 + \left(\sum_{i\in B} Q_{Li}^{st}\right)^2} + S_{loss\&spare}^{st},\ \forall i\in B \quad (4)$$

where $S_{Gi,\max}^{st}$ is the apparent power generation capacity at bus i when operating at state st, B is the set of all island buses, P_{Li} and Q_{Li} are the active and reactive load power at bus i, respectively and $S_{loss\&spare}^{st}$ is the apparent power loss and spare capacity requirements for the IMG when operating at state st. The spare capacity is intended to account for the ability of the microgrid to respond to unexpected and sudden increases in its local power demand, i.e., spinning reserve. In this work, the apparent power loss and spare capacity are considered to be 10% of the IMG demand [19].

B. Objective Functions

The three objectives of the proposed droop-controlled IMG optimum reconfiguration problem formulation are:

1) Fuel Cost Minimization: From the energy cost point of view, the optimal operation of the IMG system can be achieved by minimizing its total generation cost. If the IMG distribution feeders were lossless, the IMG configuration would have no effect on its total generation cost. However, in distribution systems IMGs the system configuration must be taken into account and a special procedure must be developed to choose the optimal configuration that minimizes the IMG total generation cost. Unlike conventional distribution systems, in IMG systems the energy cost minimization problem cannot be reduced to a loss minimization problem as the cost of the energy lost is dependent on the different DG units' characteristics (i.e., fuel type, consumption rate and fuel price); as well as the system voltage profile. In other words, if the problem is casted as a loss minimization problem, the solution will always be the configuration with the highest possible voltage profile, i.e., to decrease the current in the feeders. However, this solution does not take into account the fact that in IMG systems the reactive power support needed to maintain such a voltage profile has to come from the same DG units producing island's active power demand. Hence, such reactive power support may come on the expense of sacrificing active power generation capacity from a generator with low running cost and accordingly increasing the overall island generation costs. Accordingly, the first objective in the proposed reconfiguration problem is to minimize the IMG total generation cost. In order to account for the uncertainty and variability associated with the output power of renewable DG as well as the load variability in the calculation of the IMG total generation cost, the probabilistic IMG model developed in Section II-A is incorporated in the objective function as follows:

$$\min.\, f_1\left(X^{sw}\right) = \sum_{st}^{n_{states}}\left(\sum_{i\in B}\left(C_i\left(P_{Gi}^{st}\right)\times\sigma_i\times P_{Gi}^{st}\times\rho^{st}\right)\right) \quad (5)$$

where P_{Gi}^{st} is the active power produced by the DG unit connected to the ith bus at microgrid state σ_i,σ_i is the fuel price for the DG unit connected to the ith bus, ρ^{st} is the probability of microgrid state st, $C_i\left(P_{Gi}^{st}\right)$ is the fuel consumption of the DG unit connected to the i^{th} bus at microgrid state st as a function of its active power generation, and n_{states} is the number of IMG admissible states. X^{sw} is the control vector representing the open and close states (shown by 0 and 1, respectively) of the N_{sw} switches in the system given by

$$X^{sw} = [sw_1, sw_2\ldots, sw_{N_{sw}}]. \quad (6)$$

2) Loadability Maximization: The voltage security problem is associated with the increase of system demand beyond certain limits leading to the disappearance of the system steady-state equilibrium point [20], [21]. As such the overall IMG operational limit can be closely associated with the voltage stability of the network [22], [23]. Hence, the incorporation of voltage collapse criterion in the selection of the IMG configuration is important to maximize the distance of the operating point to voltage collapse, which in turns increases the system robustness against possible contingencies. The voltage security margin quantifies the proximity of an IMG state to the point of voltage collapse. The point at which the system steady-state solution disappears (i.e., point of voltage collapse) is known as a static bifurcation point. For a linearly increasing load, with i representing the scalar load factor, assuming an increase in the generation capacity to match the load increase, the disappearance of the system steady-state solution with an increasing $\lambda\in\Re$ can be related to the appearance of a singularity in the Jacobian matrix of the power flow equations describing the droop controlled IMG. This type of bifurcation is known as saddle node bifurcation (SNB). Moreover, considering the capacity limits of the different DG units in the IMG, a reduced static voltage stability margin might result. In this case, the disappearance of the system equilibrium can arise instantaneously with a sudden jump to instability as the capacity limit of the system equipment is reached. This type of bifurcation is known as limit induced bifurcation (LIB). In droop controlled IMG the LIB can be related to the shortage of active power supply and/or reactive power supply. Accordingly, in this work the second objective function of the proposed reconfiguration problem level is to maximize the voltage security margin. This is achieved by maximizing the possible loading margin from the current loading point for each IMG state i. In order to consider the stochastic nature of the IMG generation and demand, the different IMG states are weighted according to their probabilities. Hence, the second objective function can be given as

$$\max . f_2\left(X^{sw}\right)=\sum_{st}^{n_{states}}\left(\lambda_m^{st}-\lambda_c^{st}\right)\times\rho^{st} \tag{7}$$

where λ_m^{st} is the maximum possible load factor of the IMG at state st, and λ_c^{st} is the current load factor of the IMG at state st. Further details about the maximum loadability calculation and maximization of droop-controlled IMG systems can be found in [23].

3) Switching Operation Minimization: Modifying the configuration of any electric distribution network entails some inherent costs pertaining to the maintenance requirements and the shortened lifetime of the switches as well as the need for dispatching technicians in the case of non-automated systems. Hence, minimizing the number of switching operations reduces the time and operational cost needed for implementing the required IMG configuration. Accordingly, the third objective function in the proposed problem formulation can be given as

$$\max . f_3\left(X^{sw}\right)=\sum_{u}^{N_{sw}}\left|sw_u-sw_u^0\right| \tag{8}$$

where sw_u^0 is the status of the uth switch before reconfiguration (i.e., equals 1 for a closed switch and 0 for open switch).

C. Problem Constraints

The proposed droop-controlled IMG optimum reconfiguration problem is subjected to the following constraints:

1) Power Flow Constraints: In the droop control structure, the active power sharing is achieved by drooping the frequency of the DG unit output voltage as generated active power by the DG unit increases. Similarly, the magnitude of the DG unit output voltage is drooped as the generated reactive power by the DG unit increases [3]. Accordingly, for a droop-controlled DG unit connected to bus i, the DG output voltage frequency, ω, and magnitude, $|V_i|$, can be given as

$$\omega=\omega_i^*-m_{pi}\times P_{Gi} \tag{9}$$

$$|V_i|=|V_i|^*-n_{qi}\times Q_{Gi} \tag{10}$$

where ω_i^* and $|V_i|^*$ are the DG unit output voltage frequency and magnitude at no-load, respectively, m_{pi} and n_{qi} are the active and reactive power static droop gains, respectively, and P_{Gi} and Q_{Gi} are the injected active and reactive power by the DG unit, respectively. The static-droop characteristics given by (9) and (10) show that droop control provide a measure of negative proportional feedback that controls the DG units' active and reactive power generation and ensures that the different DG units in the island are producing voltages with the same steady-state angular frequency, i.e., system steady-state angular frequency. Accordingly, the steady-state operating point of the droop controlled IMG depends on the static droop characteristics of the different DG units in the island.

The overall steady-state behavior of droop-controlled IMGs is modeled by a set of power flow equations. Unlike conventional power flow formulations, power flow equations for a droop-controlled IMG have the following characteristics: 1) the power generated by droop-controlled DG units is determined based on the DG unit static droop characteristics set by (9) and (10) and cannot be pre-specified prior to the solution of the power flow equations; 2) a droop-controlled IMG has no slack bus capable of maintaining a constant system frequency, as such the steady-state frequency of the system is not pre-specified and is one of the power flow variables [4]. Accordingly, the set of power flow equations that reflect the special philosophy of operation of a droop-controlled IMG can therefore be formulated as follows: for each droop bus $i \in B_{droop}$, there are two mismatch equations:

$$\begin{aligned}&\frac{1}{m_{pi}}\times\left(\omega_i^*-\omega\right)-P_{Li}\\&\quad=\sum_{k\in B}\left(|V_i|\times|V_k|\times|Y_{ik}|\times\cos\left(\theta_{ik}+\delta_k-\delta_i\right)\right)\end{aligned} \tag{11}$$

$$\begin{aligned}&\frac{1}{n_{qi}}\times\left(|V_i|^*-|V_i|\right)-Q_{Li}\\&\quad=-\sum_{k\in B}\left(|V_i|\times|V_k|\times|Y_{ik}|\times\sin\left(\theta_{ik}+\delta_k-\delta_i\right)\right)\end{aligned} \tag{12}$$

where B_{droop} is the set of all droop-controlled buses in the island, B is the set of all island buses, P_{Li} and Q_{Li} are the active and reactive load power at bus i, respectively; Y_{ik} and θ_{ij} are the frequency dependent Y-bus admittance magnitude and angle respectively, and δ_i is the voltage angle at bus i. Dispatchable DG units operating in droop-controlled mode provide the energy buffering required for enabling islanded operation [19], [24]. On the other hand, renewable energy resources are locally controlled in order to track their maximum power operating point and are therefore represented as PQ buses in the IMG model. The power mismatch equations for PQ nodes are similar to conventional power flow formulations [4]. Accordingly, for each state st, the number of mismatch equations describing the power flow constraints for the IMG at certain loading condition is 2 $\times n_{bus}$-equations comprising the 2 $\times n_{bus}$-power flow state variables and n_{bus} is the number of buses in the IMG system. The angle of an arbitrary bus is set to zero so that it can be taken as the system reference. Hence, the power flow constraints for the proposed IMG optimal reconfiguration problem can be given as

$$F_\ell^{st}\left(h_\ell^{st},\tau^{st},\lambda_\ell^{st}\right)=0 \qquad \forall st\in\{1,2,\ldots,n_{states}\},\forall\ell\in\{c,m\} \tag{13}$$

where $F_{\ell}^{st}(.)$ are the power flow equations of the IMG at state st and loading condition ℓ, h_{ℓ}^{st} is the vector of state variables for the IMG at state st and loading factor ℓ including system frequency, voltage magnitudes, and angles, subscripts c and m indicate the current and maximum loading points, respectively, and τ^{st} is vector of droop settings variables for the droop controlled DG units in the IMG at state st, given as

$$\tau^{st} = \left\{\tau_j^{st} | \forall j \in B_{droop}\right\} \tag{14}$$

and

$$\tau_j = \left[\omega_j^*, |V_j|^*, m_{pj}, n_{qj}\right]. \tag{15}$$

2) DG Capacity Constraints: The generated powers by a droop-controlled DG unit connected to bus j in an IMG system, P_{Gj} and Q_{Gj}, follow the droop relations given in (9) and (10) up till the DG units' maximum active and reactive power generation limits, $P_{Gj,\max}$ and $Q_{Gj,\max}$, respectively. Beyond $P_{Gj,\max}$ the DG unit active power generation is not allowed to follow the droop relation, given by (9), and the DG is transformed to inject a constant amount of active power set at the violated limit (i.e., $P_{Gj,\max}$). Similarly, beyond $Q_{Gj,\max}$ the DG unit reactive power generation is not allowed to follow the droop relation, given by (10), and the DG is transformed to inject a constant amount of reactive power set at the violated limit (i.e., $Q_{Gj,\max}$). The relationships governing the DG units active and reactive power generation capabilities can be given as

$$P_{Gj,\max} = S_{Gj,\max} \tag{16}$$

$$Q_{Gj,\max} = \sqrt{\left(S_{Gj,\max}\right)^2 - \left(P_{Gj,\max}\right)^2}. \tag{17}$$

In order to model the behavior of DG units as they reach their maximum generation capability in the proposed problem formulation, a set of nonlinear complementary constraints have been adopted. The nonlinear complementary constraint problem, as defined in [5] and [22], is finding the vector $\partial \in \Re^n$ such that for the given mappings $A(\partial) : \Re^n \to \Re^n$ and $B(\partial) : \Re^n \to \Re^n$

$$A(\partial) \geq 0, \quad B(\partial) \geq 0, \quad A(\partial) \times B(\partial) = 0. \tag{18}$$

With the notation "$\perp$" meaning complement, (18) can be written as

$$0 \leq A(\partial) \perp B(\partial) \geq 0. \tag{19}$$

Accordingly the complementary constraints modeling the behavior of droop controlled DG units as they reach their maximum generation capacities can be given as follows:

$$0 \leq S_{Gj,\max} - P_{Gj} \perp \frac{1}{m_{pj}} \times \left(\omega_j^* - \omega\right) - P_{Gj} \geq 0 \tag{20}$$

$$0 \leq \sqrt{\left(S_{Gj,\max}\right)^2 - \left(P_{Gj}\right)^2} - Q_{Gj} \perp \frac{1}{n_{qj}} \times \left(|V_i|^* - |V_i|\right) - Q_{Gj} \geq 0. \tag{21}$$

The complementary constraints in (20)–(21) means that the active and reactive power generation of the DG unit is either following the droop characteristics given by (9) and (10) or set at the DG limits, $P_{Gj,\max}$ and $Q_{Gj,\max}$, given by (16) and (17).

Hence, the droop controlled DG units' capacity constraints for the proposed IMG optimal reconfiguration problem can be given as

$$0 \leq S_{Gj,\max}^{st} - P_{Gj,\ell}^{st} \perp \frac{1}{\tau_j^{st}(3)} \times \left(\tau_j^{st}(1) - \omega_{\ell}^{st}\right) - P_{Gj,\ell}^{st} \geq 0 \tag{22}$$

$$0 \leq \sqrt{\left(S_{Gj,\max}^{st}\right)^2 - \left(P_{Gj,\ell}^{st}\right)^2} - Q_{Gj,\ell}^{st} \perp \frac{1}{\tau_j^{st}(4)} \times \left(\tau_j^{st}(2) - |V_i|_{\ell}^{st}\right) - Q_{Gj,\ell}^{st} \geq 0 \tag{23}$$

$$\forall st \in \{1, 2, \ldots, n_{states}\}, \forall \ell \in \{c, m\}, \forall j \in B_{droop}.$$

3) Operational Constraints: Even though some urban core networks may be configured in a meshed configuration, the large majority of electric distribution systems operate with a radial topology for different technical and economic reasons; amongst the most prominent are: 1) the facilitation of coordination and protection functions brought about by the radial configuration; 2) the reduction in the short-circuit current of electric distribution network operating in radial configuration as compared to those operating in a meshed configuration; and 3) meshed configured networks are more expensive to build compared to radially configured networks. Thus, the radiality constraint is present in almost all of operation planning and expansion problems of electric distribution networks [25], [26]. The radial configuration in which the IMG must operate should not possess any closed path with all nodes energized. To ensure the radial structure of the reconfigured IMG, in the proposed optimum reconfiguration problem, the distribution system IMG is considered as a tree (i.e., connected graph without loops). A tree of a graph consisting of n nodes is a sub-graph connected with $(n-1)$ branches. Accordingly, the topology of a network with n nodes is radial if [27]

$$\sum_i sw_{(i,j)} = n_{bus} - 1, \qquad \forall i, j \in B \tag{24}$$

where n_{bus} is the number of IMG buses.

The chosen topology must be connected to provide connectivity to all system buses (i.e., to ensure that all loads are fed). Using the following rules along with the constraint in (24), the proposed IMG optimal reconfiguration problem formulation can ensure that it obtains only radial and connected configurations [28], [29]:

- All switches that do not belong to any loop are to be closed.
- Only one switch from a common branch vector (i.e., set of elements which are common between any two loops) can be selected to be opened.
- Only one switch from a non-common branch vector (i.e., set of elements which are not common with other loops) can be selected to be open.
- All the common branch vectors of a prohibited group vector (i.e., set of common branch vectors which incident to common interior nodes) cannot simultaneously have opened switches.

Moreover, the optimal configuration of the IMG network should ensure that at all the possible system states: 1) the system voltage and frequency regulation are achieved, and 2) the branch currents do not exceed their specified limits.

Accordingly $\forall st \in \{1,2,\ldots,n_{states}\}$ and $\forall i,j \in B$ the following constraints are enforced:

$$|V_i|^{lb} \le |V_i|^{st} \le |V_i|^{\,ub} \tag{25}$$
$$\omega^{lb} \le \omega^{st} \le \omega^{\,ub} \tag{26}$$
$$I_{ij}^{lb} \le \left|I_{ij}^{st}\right| \le I_{ij}^{ub} \tag{27}$$

where the subscripts lb and ub represent the system operational lower and upper bounds, respectively. The choice of the minimum and maximum allowable values of the frequency and voltage magnitude depend on the required voltage and frequency regulation [3], [4].

D. Droop-Controlled DG Units Characteristics

Droop control schemes can be subdivided into two main subclasses depending on the availability of supervisory control. In droop-control schemes without supervisory control, the droop characteristics of the different DG units in the IMG are predetermined prior to the IMG operation based on either the DG units rated capacities or a probabilistic evaluation of the IMG operation cost. In this case, the IMG operation is completely decentralized and the DG units' droop-characteristics are not updated during the IMG operation. In droop-control schemes with supervisory control, the droop-controlled IMG operation is complemented by using a MGCC along with non-critical low bandwidth communication links. Periodic measurements of the IMG generation and loads are transmitted to the MGCC. The MGCC then uses the received data to solve the IMG OPF problem and consequently update the DG units' droop characteristics to optimally dispatch the different DG units in the IMG. The advantage of such schemes is that any failure in the MGCC or its associated communication links will not result in a failure of the IMG system; such failure will only imply lack of optimal operation and resorting back to decentralized droop control with no communication; with the settings in place at the moment of communication interruption.

In the remainder of this subsection the different methods for determining the DG units droop settings are discussed:

1) Capacity Based Droop Settings: Capacity based droop settings are the same for a given IMG irrespective of its configuration or state. These settings are calculated based on the allowable voltage and frequency regulation. The static droop gains for the DG unit connected to bus i, can be given as

$$m_{pi} = \frac{\omega^{ub} - \omega^{lb}}{P_{Gi,\max}}, \quad n_{qi} = \frac{|V_i|^{ub} - |V_i|^{lb}}{Q_{Gi,\max}} \tag{28}$$

ω_i^* and $|V_i|^*$ are selected arbitrary in order to maintain adequate power-quality levels, in terms of keeping frequency and voltage within their specified operating limits, respectively.

Generally, capacity based droop settings are capable of providing near exact active power sharing between DG units in IMGs. Nonetheless, these settings might not satisfy other system operational requirements; where the reactive power sharing between the DG units is not exact and depends on the system parameters, i.e., mismatches in the power line impedances can lead to large circulating reactive power. Moreover, capacity based droop settings can only ensure voltage regulation at the DG units' PCC. A voltage violation might still occur at some load points due to voltage drops along the feeders. Furthermore, capacity based droop settings do not consider the optimal operation in terms of minimizing the system generation costs [19], [22].

2) Optimal Decentralized Droop Settings: Optimal decentralized droop settings are designed for a given IMG configuration in order to account for the different DG units' fuel consumption characteristics as well as the stochastic nature of the IMG generation and loads in the absence of a MGCC. These droop characteristics accommodate and account for all possible IMG states. Using the probabilistic model developed in Section II-A, the droop characteristics are obtained by solving

$$Min.\quad C_1(\tau) \equiv \sum_{st}^{n_{states}} \left(\sum_{j\in B} \left(C_j\left(P_{Gj}^{st}\right) \times \sigma_j \times P_{Gj}^{st} \times \rho^{st}\right)\right) \tag{29a}$$

subject to

$$F(|V_i|^{st}, \delta_i^{st}, \omega^{st}, \tau) = 0 \tag{29b}$$
$$\tau^{lb} \le \tau \le \tau^{ub} \tag{29c}$$
$$I_{ik}^{lb} \le \left|I_{ik}^{st}\right| \le I_{ik}^{ub} \tag{29d}$$
$$|V_i|^{lb} \le |V_i|^{st} \le |V_i|^{ub} \tag{29e}$$
$$\omega^{lb} \le \omega^{st} \le \omega^{ub} \tag{29f}$$
$$0 \le P_{Gj,\max}^{st} - P_{Gj}^{st} \perp \frac{1}{m_{pj}} \times (\omega_j^* - \omega^{st}) - P_{Gj}^{st} \ge 0 \tag{29g}$$
$$0 \le Q_{Gj,\max}^{st} - Q_{Gj}^{st} \perp \frac{1}{n_{qj}} \times \left(\left|V_j^*\right| - |V_j|^{st}\right) - Q_{Gj}^{st} \ge 0 \tag{29h}$$
$$\forall st \in \{1,2,\ldots,n_{states}\},\ \forall j \in B_{droop} \& \forall i,k \in B$$

where C_1 is the IMG probabilistic cost of generation, τ is the vector of droop settings variables for the droop controlled DG units in the IMG, and $\tau^{st} = \tau, \forall st \in \{1,2,\ldots,n_{states}\}$. Accordingly, the droop characteristics obtained by solving this optimization problem change as the IMG configuration change, but are the same for all the IMG states of a given configuration.

3) Optimal Droop Settings With MGCC: In the presence of a MGCC and its associated communication infrastructure, the IMG operation is optimized at each state through the optimal selection of the DG units' droop settings for this state. In other words, the droop characteristics of the different droop-controlled DG units in the IMG are updated as the IMG state changes. Accordingly, the DG units' droop characteristics account for the differences between the IMG states in terms of the available generation and demand. In this scenario, the droop-controlled DG units' settings at a given IMG state only consider the island's cost of generation and operational constraints during the subject state. For an IMG state st, the droop characteristics of the droop-controlled DG units are determined according to the following formulation:

$$Min.\quad C_2(\tau^{st}) \equiv \sum_{j\in B} \left(C_j\left(P_{Gj}^{st}\right) \times \sigma_j \times P_{Gj}^{st} \times \rho^{st}\right) \tag{30a}$$

subject to

$$F^{st}(|V_i|^{st}, \delta_i^{st}, \omega^{st}, \tau^{st}) = 0 \tag{30b}$$
$$\tau^{lb} \le \tau^{st} \le \tau^{ub} \tag{30c}$$

$$I_{ik}^{lb} \le \left|I_{ik}^{st}\right| \le I_{ik}^{ub} \tag{30d}$$

$$|V_i|^{lb} \le |V_i|^{st} \le |V_i|^{ub} \tag{30e}$$

$$\omega^{lb} \le \omega^{st} \le \omega^{ub} \tag{30f}$$

$$0 \le P_{Gj,\max}^{st} - P_{Gj}^{st} \perp \frac{1}{m_{pj}^{st}} \times (\omega_j^{*\,st} - \omega^{st}) - P_{Gj}^{st} \ge 0 \tag{30g}$$

$$0 \le Q_{Gj,\max}^{st} - Q_{Gj}^{st} \perp \frac{1}{n_{qj}^{st}} \times \left(\left|V_j^*\right|^{st} - \left|V_j\right|^{st}\right) - Q_{Gj}^{st} \ge 0 \tag{30h}$$

$$\forall j \in B_{droop} \& \forall i,k \in B$$

where C_2 is the IMG cost of generation at the IMG state st.

III. Optimization Approach

Based on operational practices, the time frame of the reconfiguration process in distribution networks is usually seasonal or yearly [29], [30]. In other words, the optimal topology chosen by the reconfiguration approach considers an operational planning horizon of a season or a year and is implemented for such operational planning horizon. This is because yearly or seasonal configuration decreases the number of switching operations required. Therefore, this in turn reduces the likelihood of switching surges, the risk of outages, and the possibility of transient disturbances arising in the system from multiple switching operations. On the other hand, it lowers the operational cost incurred due to these switching operations [30]. Here it is worth noting that even in the cases where the anticipated islanded microgrid operational planning horizon is shorter than a season, still the reconfiguration problem is to be solved offline prior to the initiation of the islanded system and the optimal configuration is to be implemented for the entire operational planning horizon.

The proposed multi-objective problem formulation for the optimal reconfiguration of IMG systems can be converted to a single objective problem formulation with the use of weighting factors. However, a major disadvantage of this approach is that the effect of the weights is highly dependent on the system and its state; hence such dependency cannot be known till the problem is solved. Relaxing some objective by a small percentage can lead to a disproportionate reduction in its optimality [23]. Furthermore, the proposed mathematical formulation of the reconfiguration problem; is a highly complex, combinatorial, non-differentiable and constrained non-linear mixed integer optimization problem which makes it prohibitive to adopt most of the exact optimization methods to solve it [31]. On the other hand, evolutionary algorithms are well known to be suitable for solving multi-objective problems because they retain the multi-objective nature of the problem. The solution of multi-objective optimization problems is usually not unique and consists of a set of acceptable optimal solutions (Pareto-front). Also, other traditional mathematical programming techniques tend to generate Pareto optimal solutions one at a time. In contrast with such conventional techniques, an evolutionary algorithm is able to find more than one element of the Pareto optimal set in a single run, because of their population-based nature [32]. Additionally, evolutionary algorithms are less susceptible to the shape or continuity of the Pareto frontier, which are serious concerns when adopting traditional mathematical programming techniques [32]. In this work, an NSGA-II was utilized for solving the proposed problem. This method is widely used in multi-objective problems because of its reduced computational effort and faster convergence compared to other methods [33]. However, the obtained solution is no guaranteed to be the true Pareto-optimal front. Still, it is a satisfactory solution and close to the true Pareto-optima front [33]. The detailed philosophy and technique of NSGA-II is described in [33].

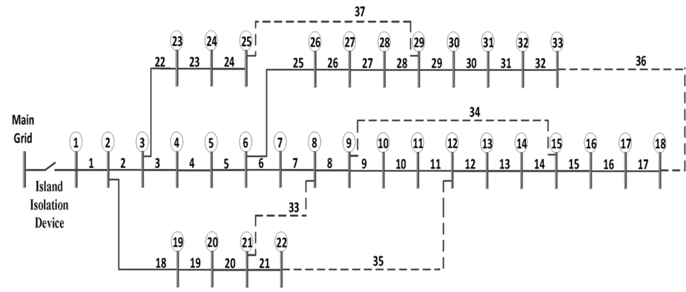

Fig. 1. 33-bus distribution test system [33].

IV. Case Studies

This section describes the testing of the proposed probabilistic reconfiguration problem formulation using the 33-bus test system shown in Fig. 1 [34]. The proposed probabilistic approach was coded in MATLAB environment. It is assumed that there is an island isolation switch at the secondary of the main substation that makes the distribution feeder capable of switching to islanded mode. In this work, the study is carried out when the feeder operates in islanded mode without consideration of the grid-connected mode of operation. The detailed types, parameters, ratings, fuel consumption rate of natural gas and modes of operation of the DG units during the islanded condition are shown in Table I. Given that all the dispatchable DG units in the system utilize the same fuel type, the system generation cost is represented in the case studies by the fuel consumption rate. Also, it is assumed that the original configuration of the distribution feeder is the one pre-switching to islanded mode (i.e., original configuration during grid-connected mode). According to the previous section discussions, three different operational scenarios are considered in this work. In the first scenario, the droop control settings are designed based on the conventional equal power sharing mechanism. In the second scenario the droop control settings are optimally designed to accommodate and account for all possible IMG states without a MGCC. The first and second scenarios do not require a communication infrastructure. In the third scenario, however, the droop control settings need a communication infrastructure to be optimized online in each IMG state via the MGCC. In order to test the convergence performance of the proposed formulation, 100 independent executions have been performed for each scenario and the most repeated solution set was selected as the actual or representative solution set (i.e., Pareto optimal configuration). The representative solution set represented 97% of all solutions for the first scenario and 94% and 96% for the second and third scenarios, respectively. The representative solution sets, for the three scenarios under consideration, are reached in near 30 iterations with a population size of 500 individuals, executing around 9000 power flow.

TABLE I
DG LOCATIONS, RATINGS, AND CONTROL MODES IN THE 33-BUS TEST SYSTEM (S_{base} = 1 MVA)

DG #	Bus #	S_{Gmax} (p.u.)	Type	Fuel Rate (scf/kWh)	Mode
1	02	2.00	Dispatchable	11.105	Droop
2	08	1.00	Dispatchable	7.806	Droop
3	09	1.00	Dispatchable	7.316	Droop
4	18	0.50	Wind	-	PQ-Unity PF
5	22	2.00	Dispatchable	11.165	Droop
6	25	1.00	Dispatchable	11.418	Droop
7	32	0.50	Wind	-	PQ-Unity PF

TABLE II
BASE CASE (SWITCHES 33, 34, 35, 36 AND 37 OPEN, $f_3 = 0$)

Droop Settings	f_1 (scf/h)	f_2 (p.u.)	V_{min} (p.u.)	V_{max} (p.u.)
Conventional	16,328.5	1.3951	0.9640	1.0403
Optimal-No Communication	15,291.1	1.2952	0.9606	1.0261
Optimal- With Communication	13,139.6	1.2054	0.9696	1.0500

Table II shows the values of the fuel consumption and system loadability as well as the minimum and maximum system voltages for the three different operational scenarios when the IMG configuration is the same as the one during normal grid-connected mode. As shown in the table, optimizing the droop control settings either with or without a MGCC caused enhancement in the rate of fuel consumption and a reduction in the system loadability. Also, as can be seen in the table, the system voltages are maintained within their specified limits in the different operational scenarios. Table II shows that there is a trade-off between the fuel consumption rate and the system loadability and a rational decision making has to be taken by the IMG operator to compromise between these two objectives. This point has been further clarified in the results presented in Tables III–V, which show the Pareto optimal configurations and the corresponding values of the objective functions as well as the system minimum and maximum voltages for the three operational scenarios, respectively. The results presented in the tables show the implications of each applied operational control scheme on the objective functions. The tables show that the minimum fuel consumption objective function value that can be obtained for the three operational scenarios using the proposed optimum configuration approach are 16,207.7, 14,299.2, and 12,590.4 scf/h, respectively. Similarly, the maximum system loadability objective function value that can be obtained for the three scenarios are 1.6817, 1.4728, and 1.6477 p.u., respectively. Compared with the base case study (i.e., results shown in Table II), one can observe that optimizing the IMG system configuration would enhance its operation by reducing the fuel consumption rate and increasing the system loadability.

In addition to the fuel consumption and the system loadability, Tables III–V show the number of switching operations required to optimally reconfigure the microgrid from its normal status during grid-connected mode of operation. As shown in the tables, the minimum possible number of switching for the three operating schemes is two switches. The results in Table III show that there are two Pareto Optimal configurations at which the minimum possible number of switches occurs. As shown in the table, changing the status of only

TABLE III
CASE STUDY #1: PARETO OPTIMAL CONFIGURATIONS-CAPACITY BASED DROOP SETTINGS

Lines Switched Out	f_1 (scf/h)	f_2 (p.u.)	f_3 (switchings)	V_{min} (p.u.)	V_{max} (p.u.)
04-12-18-32-35	16,207.7	1.6694	08	0.9877	1.0306
04-13-18-32-35	16,208.5	1.6695	08	0.9877	1.0308
03-13-18-32-35	16,210.8	1.6807	08	0.9878	1.0304
04-12-18-35-36	16,217.4	1.6522	06	0.9853	1.0316
04-13-18-35-36	16,218.1	1.6523	06	0.9853	1.0318
03-13-18-35-36	16,219.6	1.6637	06	0.9854	1.0314
18-24-34-35-36	16,246.0	1.6119	04	0.9828	1.0398
09-14-18-24-31	16,299.2	1.6817	10	0.9914	1.0414
18-34-35-36-37	16,299.5	1.5187	02	0.9711	1.0403
03-12-18-31-35	16,302.4	1.6811	08	0.9883	1.0392
20-34-35-36-37	16,306.6	1.5205	02	0.9713	1.0407
33-34-35-36-37	16,328.5	1.3951	00	0.9640	1.0403

two switches caused a decrease of the minimum possible fuel consumption from 16,328.5 scf/h to 16,299.5 scf/h and an increase of the maximum possible system loadability from 1.3951 to 1.5205. Similarly, as depicted in Table IV, the minimum possible number of two switching occurs in four Pareto Optimal configurations with a possible enhancement in the values of fuel consumption and systems loadability reached up to 15,259.5 and 1.3634, respectively. Comparing the results of Table V with those obtained in Tables III and IV, one can observe that with the same minimum possible number of switching (i.e., two switches), a significant improvement in the minimum fuel consumption and maximum system loadability occurs. Nonetheless, for all cases the significance of enhancement for either the fuel consumption or the loadability objective functions is dependent on the applied operational control scheme. For instance, the first operational scenario (conventional droop settings) has the best performance in terms of loadability and the worst in terms of fuel consumption rate. As all DG units share the active and reactive power proportional to their ratings, the system minimum voltage in the Pareto optimal configurations is found to be 0.9711, depicted in Table III. However, because of the trade-off between the two objectives, the minimum system voltages of Pareto optimal configurations for the second and third scenarios are found to be 0.9503 and 0.9696 p.u, respectively. This in turn reduces the system loadability of the second and third scenarios compared with the first scenario.

V. CONCLUSION

In this paper a new formulation for a multi-objective optimization problem has been proposed for the optimum reconfiguration of a microgrid operating in islanded mode. The objective of the proposed problem formulation is to enhance the IMG operation by choosing the optimum configuration that compromises the trade-off between the different objective functions; namely fuel consumption rate, system loadability and number of switching operations required. Three different operational control schemes (without and with communication) have been implemented in the proposed work to account for the impacts of a supervisory MGCC on the enhancement of the IMG operation. The proposed problem formulation uses a probabilistic model to integrate the load variability and the uncertainty of the renewable energy resources. To handle the trade-off between

TABLE IV
CASE STUDY #2: PARETO OPTIMAL CONFIGURATIONS- OPTIMAL DECENTRALIZED DROOP SETTINGS WITH NO COMMUNICATION

Lines Switched Out	f_1 (scf/h)	f_2 (p.u.)	f_3 (switchings)	V_{min} (p.u.)	V_{max} (p.u.)
14-19-25-35-36	14,299.2	1.0638	06	0.9581	1.0232
06-13-16-23-35	14,338.0	1.0649	08	0.9514	1.0244
05-12-16-23-35	14,531.6	1.2007	08	0.9519	1.0217
13-20-29-33-37	14,564.1	1.1923	06	0.9503	1.0314
12-18-24-28-35	14,598.2	1.2107	08	0.9651	1.0118
02-32-34-35-37	14,613.2	1.1796	04	0.9537	1.0288
02-10-17-35-37	14,632.3	1.1979	06	0.9516	1.0290
13-15-20-21-25	14,684.4	1.2194	10	0.9531	1.0223
03-13-15-21-24	14,690.8	1.2307	10	0.9571	1.0195
12-16-19-33-37	14,710.6	1.2223	06	0.9554	1.0233
12-16-33-35-37	14,750.5	1.2233	04	0.9543	1.0251
05-14-17-21-37	14,819.3	1.2455	08	0.9520	1.0295
04-14-17-21-37	14,826.6	1.2480	08	0.9518	1.0299
04-13-17-21-37	14,834.2	1.2500	08	0.9517	1.0302
03-13-17-21-37	14,861.3	1.2569	08	0.9514	1.0311
04-14-16-21-37	14,868.6	1.2609	08	0.9515	1.0313
05-14-17-35-37	14,873.5	1.2553	06	0.9528	1.0278
02-17-34-35-37	14,878.5	1.2247	04	0.9540	1.0259
05-12-16-35-37	14,913.5	1.2573	06	0.9523	1.0285
05-13-15-21-37	14,913.6	1.2700	08	0.9510	1.0330
13-24-32-33-35	15,154.8	1.3188	06	0.9750	1.0139
12-17-24-33-35	15,178.2	1.3266	06	0.9686	1.0184
13-24-33-35-36	15,188.5	1.3171	04	0.9734	1.0154
08-14-20-21-23	15,196.6	1.3347	10	0.9800	1.0121
08-14-18-21-23	15,204.2	1.3407	10	0.9800	1.0123
05-12-24-32-35	15,221.4	1.3421	08	0.9745	1.0130
12-18-32-33-37	15,226.3	1.3498	06	0.9633	1.0150
13-18-32-33-37	15,227.2	1.3508	06	0.9633	1.0151
14-18-32-33-37	15,231.7	1.3534	06	0.9635	1.0155
03-12-18-21-32	15,233.0	1.3795	10	0.9746	1.0146
03-14-18-21-32	15,236.5	1.3837	10	0.9746	1.0147
13-18-24-32-33	15,238.2	1.3989	08	0.9745	1.0134
13-18-33-36-37	15,242.7	1.3396	04	0.9614	1.0171
14-18-24-32-33	15,243.0	1.4011	08	0.9746	1.0139
14-18-33-36-37	15,245.8	1.3419	04	0.9616	1.0175
19-27-32-34-35	15,257.3	1.3733	06	0.9756	1.0222
12-33-35-36-37	15,259.9	1.2902	02	0.9602	1.0181
03-14-17-18-35	15,266.1	1.4080	08	0.9705	1.0155
03-13-17-18-35	15,267.8	1.4128	08	0.9704	1.0153
11-18-35-36-37	15,275.8	1.3583	04	0.9623	1.0173
09-14-18-24-32	15,276.4	1.4187	10	0.9746	1.0152
18-34-35-36-37	15,279.9	1.3492	02	0.9628	1.0255
10-19-35-36-37	15,285.7	1.3633	04	0.9626	1.0177
03-12-18-35-36	15,288.1	1.4059	06	0.9737	1.0153
18-24-34-35-36	15,288.7	1.3904	04	0.9737	1.0236
12-20-24-32-35	15,290.7	1.4141	08	0.9749	1.0147
33-34-35-36-37	15,291.1	1.2952	00	0.9606	1.0261
13-20-24-32-35	15,292.8	1.4150	08	0.9749	1.0148
03-13-17-19-35	15,293.0	1.4286	08	0.9700	1.0150
19-34-35-36-37	15,294.2	1.3558	02	0.9629	1.0258
10-19-24-35-36	15,299.5	1.4111	06	0.9735	1.0157
04-13-17-18-35	15,300.8	1.4332	08	0.9701	1.0148
20-34-35-36-37	15,311.9	1.3634	02	0.9631	1.0263
09-14-20-24-32	15,313.0	1.4372	10	0.9747	1.0159
05-13-17-18-35	15,319.0	1.4436	08	0.9700	1.0146
03-13-19-35-36	15,320.9	1.4221	06	0.9733	1.0159
03-12-17-20-35	15,322.9	1.4463	08	0.9698	1.0148
20-24-34-35-36	15,324.3	1.4065	04	0.9739	1.0245
03-13-16-19-35	15,328.4	1.4472	08	0.9684	1.0148
04-12-16-18-35	15,336.6	1.4534	08	0.9685	1.0146
05-12-18-35-36	15,349.0	1.4370	06	0.9734	1.0157
05-12-17-19-35	15,351.5	1.4636	08	0.9698	1.0144
04-13-19-35-36	15,365.7	1.4448	06	0.9732	1.0162
04-12-17-20-35	15,366.5	1.4693	08	0.9697	1.0144
04-13-20-35-36	15,408.5	1.4541	06	0.9731	1.0169
05-12-16-20-35	15,428.8	1.4728	08	0.9682	1.0142
05-13-20-35-36	15,436.2	1.4592	06	0.9731	1.0171

the different objectives, NSGA-II has been utilized to obtain the Pareto optimal configuration for each operational control schemes. The results show that optimizing the IMG system configuration would enhance its operation by reducing the fuel consumption rate and increasing the system loadability and the significance of such enhancement for each objective function is dependent on the applied operational control scheme and the number of switching operations implemented. For instance, the results show that the maximum system loadability is obtained when the conventional droop control settings using the equal sharing mechanism is applied. While, the minimum fuel consumption rate is obtained when a MGCC is exist. As such a rational decision making has to be taken by the IMG operator to compromise between the operational control schemes that affect significantly on the two objective functions.

TABLE V
CASE STUDY #3: PARETO OPTIMAL CONFIGURATIONS- OPTIMAL DROOP SETTINGS WITH MGCC AND COMMUNICATION

Lines Switched Out	f_1 (scf/h)	f_2 (p.u.)	f_3 (switchings)	V_{min} (p.u.)	V_{max} (p.u.)
04-12-17-24-35	12,590.4	1.4775	08	0.9893	1.0500
13-15-18-21-24	12,618.8	1.4850	10	0.9856	1.0496
04-14-17-24-35	12,620.5	1.5486	08	0.9890	1.0500
03-13-17-18-35	12,644.3	1.5520	08	0.9776	1.0500
04-14-24-35-36	12,658.6	1.4643	06	0.9836	1.0500
08-14-18-24-32	12,675.8	1.6135	10	0.9870	1.0500
05-13-16-19-35	12,687.7	1.6072	08	0.9881	1.0500
05-14-16-19-35	12,693.5	1.6124	08	0.9751	1.0498
08-13-19-24-32	12,695.3	1.6330	10	0.9775	1.0500
05-14-19-32-35	12,722.1	1.6464	08	0.9805	1.0495
13-21-32-33-37	12,739.7	1.4861	06	0.9810	1.0500
09-13-20-36-37	12,740.3	1.5125	06	0.9885	1.0500
14-24-33-35-36	12,746.1	1.3509	04	0.9845	1.0498
17-20-24-34-35	12,752.3	1.5504	06	0.9809	1.0499
04-13-19-35-36	12,778.1	1.5891	06	0.9794	1.0500
20-32-34-35-37	12,819.5	1.4201	04	0.9839	1.0500
19-34-35-36-37	12,823.2	1.3029	02	0.9712	1.0499
20-24-32-35-36	12,824.1	1.4762	04	0.9820	1.0498
03-12-18-31-35	12,842.8	1.6477	08	0.9846	1.0492
18-34-35-36-37	12,844.7	1.3431	02	0.9779	1.0500
33-34-35-36-37	13,139.6	1.2054	00	0.9696	1.0500

REFERENCES

[1] *IEEE Guide for Design, Operation, and Integration of Distributed Resource Island Systems with Electric Power Systems*, IEEE standard 1547.4, Jul. 2011.

[2] F. Blaabjerg, R. Teodorescu, M. Liserre, and A. V. Timbus, "Overview of control and grid synchronization for distributed power generation systems," *IEEE Trans. Ind. Electron.*, vol. 53, no. 5, pp. 1398–1409, Oct. 2006.

[3] N. Pogaku, M. Prodanovic, and T. C. Green, "Modeling, analysis and testing of autonomous operation of an inverter-based microgrid," *IEEE Trans. Power Electron.*, vol. 22, no. 2, pp. 613–625, Mar. 2007.

[4] M. M. Abdelaziz, H. E. Farag, E. F. El-Saadany, and Y. A.-R. Mohamed, "A novel and generalized three-phase power flow algorithm for islanded microgrids using a newton trust region method," *IEEE Trans. Power Syst.*, vol. 28, no. 1, pp. 190–201, Feb. 2013.

[5] G. Diaz and C. Gonzalez-Moran, "Fischer-Burmeister-based method for calculating equilibrium points of droop-regulated microgrids," *IEEE Trans. Power Syst.*, vol. 27, no. 2, pp. 959–967, May 2012.

[6] M. Z. Kamh and R. Iravani, "A sequence frame-based distributed slack bus model for energy management of active distribution networks," *IEEE Trans. Smart Grid*, vol. 3, no. 2, pp. 828–836, Jun. 2012.

[7] C. A. Hernandez-Aramburo, T. C. Green, and N. Mugniot, "Fuel consumption minimization of a microgrid," *IEEE Trans. Ind. Appl.*, vol. 41, no. 3, pp. 673–681, May 2005.

[8] E. Barklund, N. Pogaku, M. Prodanovic, C. Hernandez-Aramburo, and T. C. Green, "Energy management in autonomous microgrid using stability-constrained droop control of inverters," *IEEE Trans. Power Electron.*, vol. 23, no. 5, pp. 2346–2352, Sep. 2008.

[9] P. H. Divshali, S. H. Hosseinian, and M. Abedi, "A novel multi-stage fuel cost minimization in a VSC-based microgrid considering stability, frequency, and voltage constraints," *IEEE Trans. Power Syst.*, vol. 28, no. 2, pp. 931–939, May 2013.

[10] S. Conti, R. Nicolosi, S. A. Rizzo, and H. H. Zeineldin, "Optimal dispatching of distributed generators and storage systems for MV islanded microgrids," *IEEE Trans. Power Del.*, vol. 27, no. 3, pp. 1243–1251, Jul. 2012.

[11] A. Basu, A. Bhattacharya, S. Chowdhury, and S. P. Chowdhury, "Planned scheduling for economic power sharing in a CHP-based microgrid," *IEEE Trans. Power Syst.*, vol. 27, no. 1, pp. 30–38, Feb. 2012.

[12] H. Kanchev, D. Lu, F. Colas, V. Lazarov, and B. Francois, "Energy management and operational planning of a microgrid with a PV-based active generator for smart grid applications," *IEEE Trans. Ind. Electron.*, vol. 58, no. 10, pp. 4583–4592, Oct. 2011.

[13] B. Venkatesh, R. Ranjan, and H. B. Gooi, "Optimal reconfiguration of radial distribution systems to maximize loadability," *IEEE Trans. Power Syst.*, vol. 19, no. 1, pp. 260–266, Feb. 2004.

[14] L. S. M. Guedes, A. C. Lisboa, D. A. G. Vieira, and R. R. Saldanha, "A multiobjective heuristic for reconfiguration of the electrical radial network," *IEEE Trans. Power Del.*, vol. 28, no. 1, pp. 311–319, Jan. 2013.

[15] R. S. Rao, K. Ravindra, K. Satish, and S. V. L. Narasimham, "Power loss minimization in distribution system using network reconfiguration in the presence of distributed generation," *IEEE Trans. Power Syst.*, vol. 28, no. 1, pp. 317–325, Feb. 2013.

[16] A. R. Malekpour, T. Niknam, A. Pahwaand, and A. K. Fard, "Multi-objective stochastic distribution feeder reconfiguration in systems with wind power generators and fuel cells using the point estimate method," *IEEE Trans. Power Syst.*, vol. 28, no. 2, pp. 1483–1492, May 2013.

[17] Y. M. Atwa, E. F. El-Saadany, M. M. A. Salama, R. Seethapathy, M. Assam, and S. Conti, "Adequacy evaluation of distribution system including wind/solar DG during different modes of operation," *IEEE Trans. Power Syst.*, vol. 26, no. 4, pp. 1945–1952, Nov. 2011.

[18] Y. M. Atwa, E. F. El-Saadany, M. M. A. Salama, and R. Seethapathy, "Optimal renewable resources mix for distribution system energy loss minimization," *IEEE Trans. Power Syst.*, vol. 25, no. 1, pp. 360–370, Feb. 2010.

[19] H. E. Farag, M. M. A. Abdelaziz, and E. F. El-Saadany, "Voltage and reactive power impacts on successful operation of islanded microgrids," *IEEE Trans. Power Syst.*, vol. 28, no. 2, pp. 1716–1727, May 2013.

[20] W. Rosehart, C. Roman, and A. Schellenberg, "Optimal power flow with complementarity constraints," *IEEE Trans. Power Syst.*, vol. 20, no. 2, pp. 813–822, May 2005.

[21] W. Rosehart, C. Canizares, and V. H. Quintana, "Multiobjective optimal power flows to evaluate voltage security costs in power networks," *IEEE Trans. Power Syst.*, vol. 18, no. 2, pp. 578–587, May 2003.

[22] M. M. A. Abdelaziz, H. E. Farag, and E. F. El-Saadany, "Optimum droop parameter settings of islanded microgrids with renewable energy resources," *IEEE Trans. Sustain. Energy*, vol. 5, no. 2, pp. 434–445, Apr. 2014.

[23] M. M. A. Abdelaziz and E. F. El-Saadany, "Maximum loadability consideration in droop-controlled islanded microgrids optimal power flow," *Elect. Power Syst. Res.*, vol. 106, pp. 168–179, Jan. 2014.

[24] G. Diaz, C. Gonzalez-Moran, and C. Viescas, "Operating point of islanded microgrids consisting of conventional doubly fed induction generators and distributed supporting units," *IET Renew. Power Gener.*, vol. 6, no. 5, pp. 303–314, 2012.

[25] M. Lavorato, J. F. Franco, M. J. Rider, and R. Romero, "Imposing radiality constraints in distribution system optimization problems," *IEEE Trans. Power Syst.*, vol. 27, no. 1, pp. 172–180, Feb. 2012.

[26] A. M. G. Solo, G. Ramakrishna, and R. J. Sarfi, "A knowledge-based approach for network radiality in distribution system reconfiguration," in *Proc. IEEE Power Energy Soc. General Meeting*, 2006.

[27] J. Mendoza, R. Lopez, D. Morales, E. Lopez, P. Dessante, and R. Moraga, "Minimal loss reconfiguration using genetic algorithms with restricted population and addressed operators: Real application," *IEEE Trans. Power Syst.*, vol. 21, no. 2, pp. 948–954, May 2006.

[28] N. Gupta, A. Swarnkar, K. R. Niazi, and R. C. Bansal, "Multi-objective reconfiguration of distribution systems using adaptive genetic algorithm in fuzzy framework," *IET Gener., Transm., Distrib.*, vol. 4, no. 11, pp. 1213–1222, 2010.

[29] A. Zidan, M. F. Shaaban, and E. El-Saadany, "Long-term multi-objective Distribution network planning by DG allocation and feeders' reconfiguration," *Elect. Power Syst. Res.*, vol. 105, pp. 95–104, Dec. 2013.

[30] S. Yin and C. Lu, "Distribution feeder scheduling considering variable load profile and outage costs," *IEEE Trans. Power Syst.*, vol. 24, no. 2, pp. 652–660, May 2009.

[31] E. M. Carreno, R. Romero, and A. P. Feltrin, "An efficient codification to solve distribution network for loss reduction problem," *IEEE Trans. Power Syst.*, vol. 23, no. 4, pp. 1542–1551, Nov. 2008.

[32] C. A. Coello, "Evolutionary multi-objective optimization: A historical view of the field," *IEEE Computat. Intell. Mag.*, vol. 1, no. 1, pp. 28–36, Feb. 2006.

[33] K. Deb, S. Agrawal, A. Pratab, and T. Meyarivan, "A fast elitist non dominated sorting genetic algorithm for multi-objective optimization: NSGA-II," in *Proc. Parallel Problem Solving From Nature VI Conf.*, 2000, pp. 849–858.

[34] D. Singh and R. Misra, "Effect of load models in distributed generation planning," *IEEE Trans. Power Syst.*, vol. 22, no. 4, pp. 2204–2212, Nov. 2007.

Morad Mohamed Abdelmageed Abdelaziz (M'15) was born in Cairo, Egypt, on September 27, 1984. He received the B.Sc. (with honors) and M.Sc. degrees from Ain Shams University, Cairo, Egypt, in 2006 and 2009, respectively, both in electrical engineering, and the Ph.D degree in electrical and computer engineering from the University of Waterloo, Waterloo, ON, Canada, in 2014.

His research interests include dynamics, controls and analysis of microgrids and active distribution networks; integration of distributed and renewable generation, power electronics converters and their applications in smart grids.

Hany E. Farag (M'13) was born in Assiut, Egypt, on November 21, 1982. He received the B.Sc. (with honors) and M.Sc. degrees in electrical engineering from Assiut University, Egypt, in 2004 and 2007, respectively, and the Ph.D. degree in electrical engineering from the University of Waterloo, Waterloo, ON, Canada, in 2013.

Currently, he is an Assistant Professor in the Department of Electrical Engineering and Computer Science, Lassonde School of Engineering, York University, Toronto, ON, Canada. His research interests are in the areas of active distribution networks, integration of distributed and renewable energy resources, modeling, analysis and design of microgrids, and applications of multi-agent technologies in smart grids. His biography is listed in the 30th pearl anniversary edition of *Marquis Who's Who in the World* in 2012.

Dr. Farag is registered as a professional engineer (P.Eng) in Ontario.

Ehab F. El-Saadany (SM'05) was born in Cairo, Egypt, in 1964. He received the B.Sc. and M.Sc. degrees in electrical engineering from Ain Shams University, Cairo, Egypt, in 1986 and 1990, respectively, and the Ph.D. degree in electrical engineering from the University of Waterloo, Waterloo, ON, Canada, in 1998.

Currently, he is a Professor in the Department of Electrical and Computer Engineering, University of Waterloo. His research interests are smart grids operation and control, power quality, distributed generation, power electronics, digital signal processing applications to power systems, and mechatronics.